8th Japan-China-Korea Workshop on Microgravity Sciences
for Asian Microgravity Pre-Symposium

System Engineering Analysis and Optimization of a Parabolic Flight Experiment for Thermophysical Property Measurement under Microgravity

Keigo KAKIKURA [1], Koji FUKAGATA [2] and Taketoshi HIBIYA [1]

Abstract

In order to perform microgravity experiments successfully, analysis of the experiments is strongly recommended by a primary investigator from the viewpoint of system engineering. Thermophysical property measurement using the PFLEX (Parabolic Flight Levitation Experiment facility) under the microgravity condition was analyzed. The experiment system was decomposed into subsystem and component levels, and a bottle neck for the experimental system was extracted, i.e. gravitational change as high as 1.5G during the climb-up phase. The numerical simulation of temperature and velocity fields of gas flow around the high temperature sample indicates that the conventional method for oxygen partial pressure control, i.e. a gas flow method in open space, can not control oxygen partial pressure under the 1.5G condition. Instead, we propose a new control model, i.e. gas flow at a velocity over 0.5 m/s using a glass tube, and CFD (computational fluid dynamics) verified that this model shows a good controllability of oxygen partial pressure even under the 1.5 G condition. The CFD program is more effective than empirical methods on board the aircraft, so as to optimize a gas flow condition.

1. Introduction

1.1 Variable Gravitational Acceleration

Recently many microgravity experiments have been carried out using the International Space Station (ISS), a space shuttle, a sounding rocket, a jet plane in parabolic flight and a drop tower. Among them, experiments using a jet plane, sounding rocket and a drop tower are superior from the viewpoints of cost-performance and the preparation period of experiments, even though the microgravity duration is rather short. In particular, the parabolic flight of a jet plane can supply a variable gravitational acceleration level depending on the attitude of the aircraft, i.e. change of air drag due to a variable pitch angle and a centrifugal force by a bank flight, whereas we can obtain the following constant microgravity conditions, such as 10^{-5} G within a drop tower, 10^{-4} G aboard the ISS and 10^{-2} G by a usual parabolic flight. Nakamura et al. calculated the critical Rayleigh number for the breakout of the buoyancy effect on thermal conductivity measurements of mercury using a variable gravitational acceleration aboard a jet plane[1]. The concept of variable gravity has also been important for combustion science; numerical and experimental studies were performed using parabolic flights[2].

We measure thermophysical properties of metallic melts using electromagnetic levitation (EML) under the microgravity condition using the Parabolic Flight Levitation EXperiment facility (PFLEX)[3] with Gulf Stream II. The melt density, viscosity and the oxygen partial pressure (Po_2) dependence of surface tension were investigated. Since surface tension of molten metals is sensitive to Po_2, gas flow of an ambient atmosphere must be controlled precisely, regardless of gravitational acceleration condition.

A parabolic flight experiment system is complex from several viewpoints, such as gravitational acceleration, facilities, operations, human activities and so on. For example, electric power is not available when the plane stays on the apron but can be supplied after starting the engines. Gravitational acceleration changes in the range from 10^{-2} to 1.5 G, depending on the attitude of a jet plane, such as the pitch angle. Acceleration of 1.5 G is inevitably required to obtain the longest microgravity condition, i.e. a 45-degree parabolic flight. Levitation must be started from a horizontal flight stage through a hyper-gravity condition, so as to fully utilize microgravity condition for 20 s. However, this hyper-gravity can cause fly-out of a levitated droplet from the coil system. In order to assure stable levitation during this hyper-gravity condition, a discussion is necessary between experimenters and pilots[4], i.e. selection of a pitch angle during the climb-up phase. Human activities are limited due to safety reasons. Experimenters are sometimes confused due to the physiological reaction of the human body caused by gravity change. These are constraints for carrying out parabolic flight experiments. Overcoming these problems, microgravity environment for about 20s is available.

---

1 Graduate School of System Design and Management, Keio University, 4-1-1 Hiyoshi, Kohoku-ku, Yokohama, Kanagawa 223-8526, Japan
2 Graduate School of Science and Technology, Keio University, 3-14-1 Hiyoshi, Kohoku-ku, Yokohama, Kanagawa 223-8522, Japan
(E-mail: t.hibiya@sdm.keio.ac.jp)
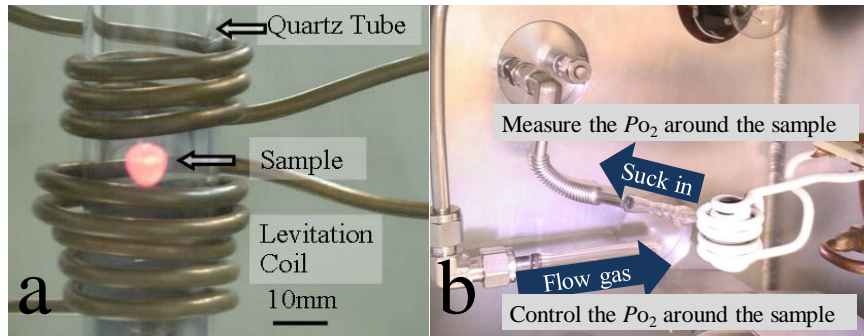
Fig. 1　Apparatus for levitating and heating the melt and for controlling the ambient gas around the melt. (a) Po_2 is controlled and measured through the glass tube inside the coil in the ground-based experiment. (b) Po_2 is controlled by gas flow to the melt and measured by sucking the ambient gas through an open space outside the coil during the microgravity experiment.

1.2.　System Engineering Analysis

From the viewpoint of the system engineering, we are required to use the precious microgravity condition effectively considering the various constraints. In order to adapt the ground-based experimental system to the microgravity condition, the experimental design should be modified to meet the parabolic flight conditions and constraints. Thus, we should optimize the experimental procedure. This means to assure the final purpose of the experiment and to compromise several different requirements from multiple stakeholders. However conventionally, a discussion from the viewpoint of system engineering has not been familiar to scientists, because sometimes they do not show interest in a system engineering analysis for experiments, being responsible only for experiments from scientific viewpoint. On the other hand, for space experiments, such as that aboard the ISS, space shuttles and sounding rockets, a system engineering approach has been adapted by agency officials and engineers, i.e. system analysis through a system requirement review, a preliminary design review and a critical design review[5]. Especially for aircraft experiments, the analysis of experiments has not been performed from a system engineering viewpoint except for a small discussion meeting between scientists and engineers from Diamond Air Service (DAS), the operating company, a manual issued by DAS, articles on hardware and lessons-learned from scientists[6]. This is because an experimental scale is comparatively small and scientists can manage the experiment themselves based on their experience even though a method is not analytical.

1.3.　Optimization of Oxygen Flow Control

Although the static effect of the microgravity condition has been reported on the measurements of diffusion constant[7] and thermal conductivity[1], there are few reports which focus on the effect of time-dependent gravitational acceleration on

thermophysical property measurements. In the PFLEX experiment, there is a significant difference between ground-based and flight experiments, when control of oxygen partial pressure is discussed. During surface tension measurements, Po_2 was usually controlled by a gas flow. However, in these cases, the fluid dynamical effect of gravity change from 1.5 G to 10^{-2} G on gas transport during experiments has not yet been clarified. Another problem is g-jitter due to several unidentified events.

These two phenomena are predicted to affect the measurement accuracy and precision for thermophysical properties. In particular, the behavior of the ambient buoyancy convection depending on gravitational acceleration should be considered with reference to oxygen transport.

Figures 1a and **1b** show the levitation apparatuses for use in ground-based and parabolic flight experiments, respectively. For ground-based experiments, in order to change the Po_2 around the melt sample, oxygen-controlled gas flows from top to bottom through a quartz glass tube placed within the levitation coil as shown in **Fig. 1(a)**. The Po_2 is measured at the bottom of the tube. For parabolic flight experiments, a glass tube is not applicable and Po_2 is controlled by gas flow from a nozzle to the melt surface and observed by sucking the gas through an open space as shown in **Fig. 1(b)**, because an automated rotating sample exchanger is employed and located just beneath the coil. This device enables multiple samples processing in a series of parabolic flights, which is cost effective. However, gas flow through a glass tube is not applicable. If the glass tube is installed, the sample exchanger interferes with the glass tube.

1.4.　Objective of the Present Study

In the present study, we analyze the PFLEX project from two viewpoints. Firstly, we analyze an experimental design and procedure from the viewpoint of system engineering and secondly, the effect of the change of the gravitational acceleration through computational fluid dynamics. We reveal that the present Po_2 control method has a lack of robustness
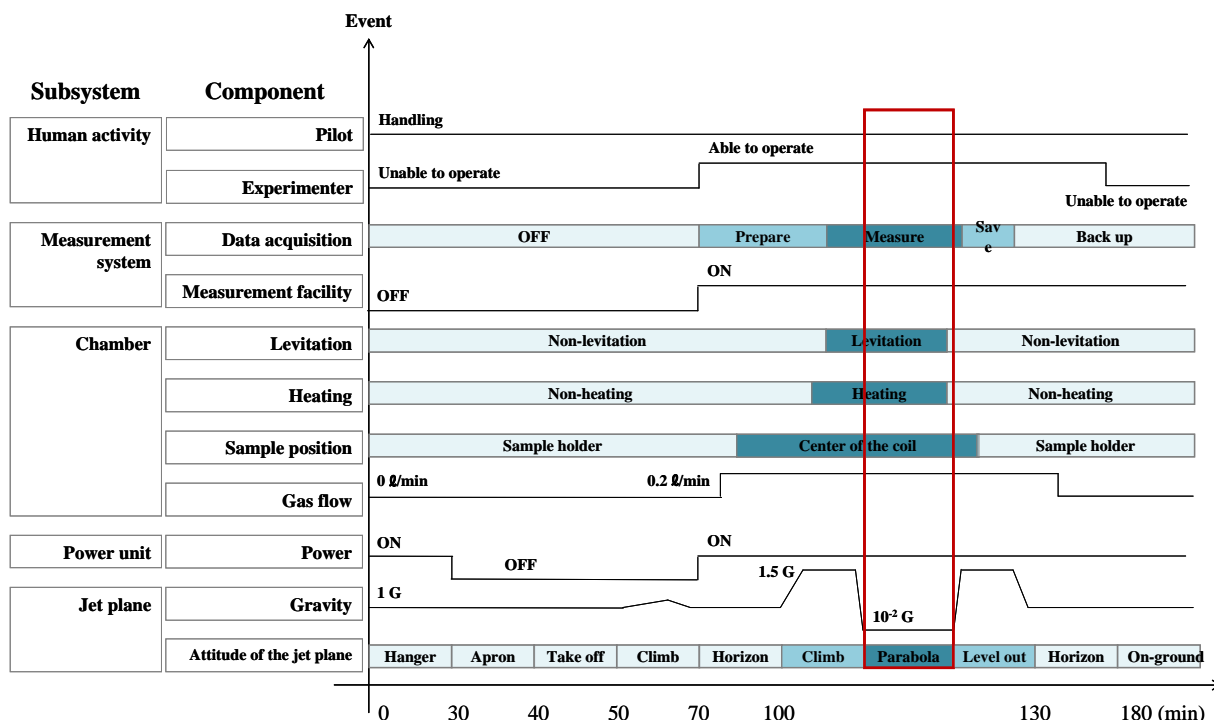
Fig. 2 The subsystems and components of the PFLEX experiment system and the time-dependent state of each component. The relations between each component are clarified. Parabolic flight experiment is depicted by a red rectangular.

against the change of gravitational acceleration. Finally, a new Po_2 control method is proposed and confirmed that the new method has a good controllability of Po_2.

2. System Engineering Analysis

A parabolic flight experiment is reviewed and the inevitable problems are extracted through system engineering analysis.

2.1 Surface Tension Measurement

The PFLEX assures a surface tension measurement under contamination-free conditions, because a containerless levitation technique is employed. Surface tension is calculated by analyzing the surface oscillations. Although calibration is required for the ground-based measurement due to deformation of a droplet, this is not the case for the microgravity experiment, because an ideal spherical shape of the droplet is assured and therefore the Rayleigh's equation is applicable without calibration. The details of the scientific purpose and processes of the PFLEX experiment are reported elsewhere[3].

2.2 Parabolic Flight Experiment System

Compared with a ground-based experiment, a parabolic flight experiment has much complexity in operations due to the constraints caused by performing experiments aboard an aircraft. Therefore, analysis of the experiment from a viewpoint of

system engineering becomes necessary to understand the characteristics of each event according to aircraft attitude, such as gravity, power, gas flow and so on. The analysis corresponds to describing CONOPS (concept of operations) in the terminology of system engineering.

All events of a parabolic flight are governed by a change of aircraft attitude. **Figure 2** shows the state of the events using the words "subsystem" or "component" depending on aircraft attitude. The attitude of the aircraft, which plays a role as if it were an independent variable, is described on the horizontal axis, and the events which depend on the attitude of the aircraft, such as the power unit, the chamber, measurement system and human activity are described on the vertical axis. These vertical axis events can be defined as a "subsystem" of a parabolic flight experiment system. Furthermore, these subsystems are decomposed into "components" and chamber is further decomposed into levitation, heating, sample position and gas flow. The state of the components should be analyzed with the attitude of the jet plane, so as to optimize the experimental operation.

According to **Fig. 2**, the PFLEX experiment using a jet plane has several problems. For example, the experimenters are supposed to operate the facilities only after entering the horizontal flight mode because they are required to be seated at all times except during the horizontal flight phase. None of the
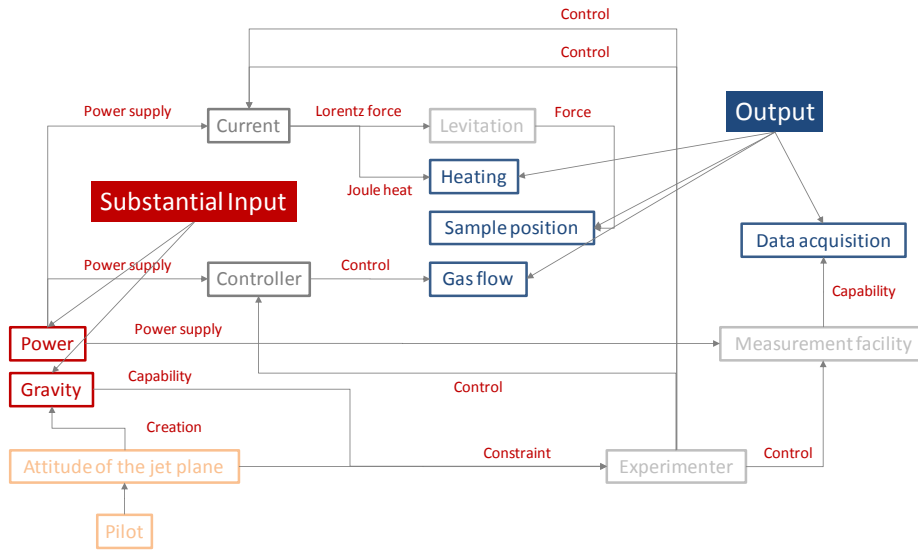
Fig. 3   The architecture among the components of PFLEX system.

facilities do work during the take-off and before entering a horizontal flight, because power is available only after entering the horizontal phase in the present experiment. These two constraints are derived from the attitude of the aircraft. The relation between the experimenters and the aircraft attitude, and also the relation between the power unit and the aircraft attitude are clarified by analyzing the experiment from the operational viewpoint. Similarly, the relation between the gravitational acceleration and the aircraft attitude is analyzed. The aircraft is accelerated from 1 G in horizontal flight to 1.5 G in the climbing phase and enters the microgravity condition of 10^{-2} G immediately. The aircraft is also affected by several unidentified events, such as air drag, human activities and so on. The unidentified events also affect g-jitter during the microgravity condition.

2.3   System Architecture

Among the components in **Fig. 2**, we are possible to understand using the concept of architecture, what the bottleneck of the PFLEX system is. **Figure 3** shows the architecture among the components of the PFLEX system. The components and the relations are represented by boxes and arrows. The inevitable gravity change is caused by the attitude of a jet plane; in another word, that is caused by a pilot. Thus, one of the input factors of the system is a pilot. However the gravity change, the attitude of the jet plane and a pilot can be defined to be equal parameter. Therefore, we define gravity change as one of the substantial inputs. Another substantial input is power, because voltage and current are independent from the gravity. These two inputs affect other components. As a
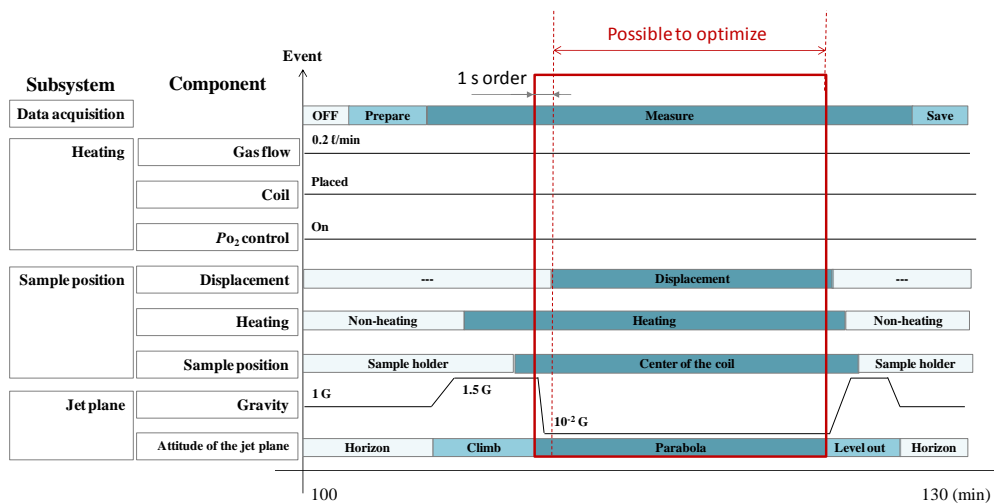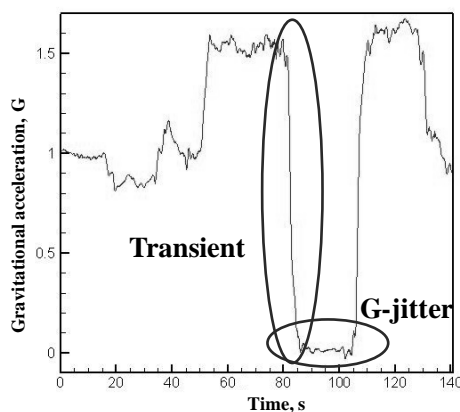

Fig. 4   Time sequence of the state of "Data acquisition", "Heating" and "Sample position" with the attitude of a jet plane.

result, "Heating", "Sample position", "Gas flow" and "Data acquisition" are led as out puts of the PFLEX system.

Figure 4 shows the time sequence state of the above mentioned components of the four subsystems. Among them, "Data acquisition" is negligible to consider the effect of gravity because voltage and current are independent from gravity. Furthermore, "Data acquisition" is negligible when considering the effect of power, because power can be supplied enough before parabolic flight, as shown in **Fig. 2**. Therefore, in order to optimize the PFLEX system, we should consider only "Heating", "Sample position" and "Gas flow", which are contained by a chamber subsystem. Similarly, by analyzing the components, it is revealed that only the displacement of the sample is internal of the parabolic flight phase. However, this time scale is short against the microgravity condition and inevitable constraint. Thus, we can neglect them and the PFLEX system has been predicted to be optimized already. However, "Gas flow" should be considered because this is invisible phenomenon and has not been verified yet. Therefore, we should only consider the "Gas flow" by CFD (computational fluid dynamics) from the gravity viewpoint. It should be verified, whether the gravity change would affect the experimental result or not. Buoyancy convection is enhanced under 1.5 G condition and vanish under microgravity condition. There might be an aftereffect of gravity change on Po_2 control from a viewpoint of "gas flow": see **Fig. 2**.

2.4 Gravitational Acceleration Change

The gravitational acceleration change might affect Po_2 control, because oxygen is transported by gas flow. Buoyancy convection is estimated to be strong in the PFLEX experiment, because the molten metal sample has a high temperature of over 1000 K.

Figure 5 shows an example of the gravitational acceleration change observed for 140 s during a parabolic flight experiment including the microgravity phase as follows: horizontal flight (0-20 s), shallow dive (20-35 s), climb (35-85 s), microgravity (85-105 s), leveling-out (105-130 s) and horizontal flight (after 130 s). Although we hope to obtain the ideal microgravity condition to observe the melt oscillation precisely, the microgravity condition is not necessarily ideal due to two kinds of gravitational changes. One is the rapid change of gravitational acceleration from 1.5 G to microgravity condition and another one is the gravitational fluctuation in microgravity phase, i.e. "g-jitter".

The strong buoyancy convection is created by the large gravitational acceleration of 1.5 G in the climb phase. Although a microgravity condition can be obtained soon after starting a parabolic flight, a "transient" behavior could appear and result in a delay of hydrodynamic response. Although this effect could be short, the transient behavior should be made clear, so as to fully utilize the microgravity condition of 20 s. The gravitational acceleration is oscillating even in the microgravity condition due to the vibration of the aircraft, i.e. g-jitter. Depending on the gravity change, gas flow around the high temperature melt could also oscillate and affect the Po_2 control. Transient behavior and g-jitter effect for gas flow is invisible as long as visualization using a smoke technique is not applied and this technique cannot be employed for thermophysical property measurement in a contamination-free condition. In this study, we simulate the gas flow around the high temperature melt sphere using computational fluid dynamics and analyze the effect of gravitational acceleration for gas flow.
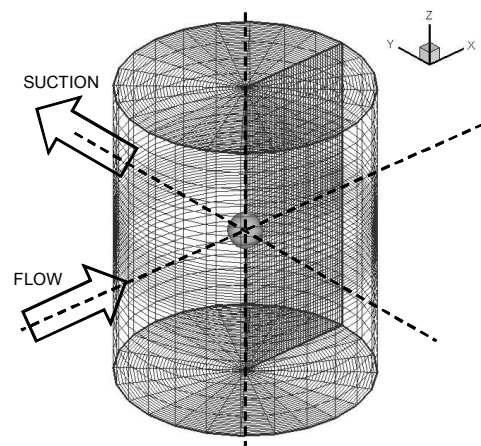

Fig. 5 Gravitational acceleration change observed for 140 s during a parabolic flight experiment. Horizontal flight (0-20 s), shallow dive (20-35 s), climb (35-85 s), microgravity (85-105 s), leveling-out (105-130 s) and horizontal flight (after 130 s). G-jitter appears in the microgravity phase.

Fig. 6 Numerical simulation model: gas flows to a sample surface and is sucked out.

3. Numerical Simulation

The effects of gravitational acceleration level on gas flow around the high temperature melt are numerically simulated using the Boussinesq approximation.

3.1 Numerical Procedure (conventional Model)

Figure 6 shows the numerical model. A high temperature solid sphere is placed at the center of the cylindrical container having two windows for gas inlet and outlet. The model mimics the chamber of the PFLEX. The diameter and temperature of solid sphere and the entrance and suction gas flow rates are equal to those of the PFLEX, i.e., 4 mm, 1300 K and 0.2 l/min, respectively.

The governing equations for the motion of an incompressible fluid flow are the continuity, Navier-Stokes, and energy equations:

$$\nabla \cdot \mathbf{u} = 0 \tag{2}$$

$$\frac{\partial \mathbf{u}}{\partial t} = -(\mathbf{u} \cdot \nabla)\mathbf{u} + \frac{1}{Re}\nabla^2\mathbf{u} - \nabla p + \frac{Gr}{Re^2}T\mathbf{g} \tag{3}$$

$$\frac{\partial T}{\partial t} = -\nabla \cdot (\mathbf{u}T) + \frac{1}{Re \cdot Pr}\nabla^2 T \tag{4}$$

and

$$Re = \frac{DU}{\nu}, \quad Gr = \frac{g\beta(T_s - T_g)D^3}{\nu^2}, \quad Pr = \frac{\nu}{\alpha} \tag{5}$$

Here, the equations are nondimensionalized by using the sphere diameter D, the inlet gas velocity U, the kinematic viscosity of fluid ν, the gravitational acceleration g, the volume expansion ratio β, the temperature of sphere T_S, and the temperature of ambient gas T_g. The Reynolds number, the Grashof number and the Prandtl number are defined as shown in eq. (5), where α is the thermal diffusivity.

The computational domain has a radius of 2.5 D and a length of 8.25 D, as shown in **Fig. 6** and no-slip boundary condition is applied at all boundaries except for two windows; four meshes
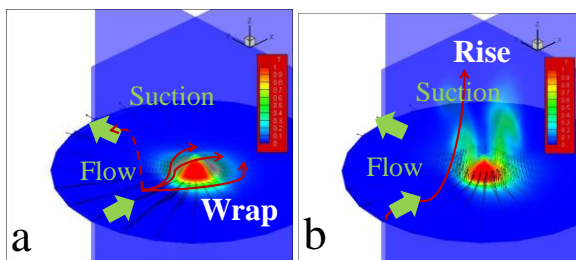

Fig. 7 Velocity and temperature fields around (a) the high temperature sphere under microgravity and (b) 1.5 G condition.

on the wall surface are assigned for the gas inlet and outlet. The number of computational cells is 40 × 24 × 40 for the radial, azimuthal, and axial directions, respectively. Equally spaced cells are used in the azimuthal direction and unequally spaced cells are adopted in the other directions. The time integration of the discretized equation is achieved by using the Euler explicit method. The HSMAC (Highly Simplified Marker And Cell) method for the pressure coupling and the energy-conservative finite difference method[9] for spatial discretization are used. Unsteady flows under the 1.5 G and microgravity conditions are simulated at the Reynolds, Prandtl and Grashof numbers of 85, 0.71 and 14700, respectively.
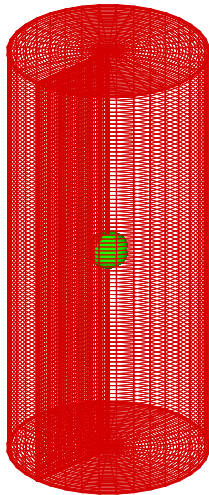
3.2 Numerical Result (Conventional Model)

Figure 7 shows the velocity and temperature fields at the same time instant under different gravitational accelerations. Convection due to buoyancy is found to be weak under the microgravity condition **(Fig. 7a)** and strong under the 1.5 G condition **(Fig. 7b)**. The gas is observed to wrap the sphere under the microgravity condition and sucked out through the outlet window, as shown by a red line in **Fig. 7a**. Furthermore, an ambient gas rises up strongly and gas beneath the sphere is forced to rise up due to strong buoyancy convection at 1.5 G condition. Thus, inlet gas is unable to reach the sphere surface, as shown by a red line in **Fig. 7b**.

Under the microgravity condition, the inlet gas reaches and wraps the sphere, whereas the Po_2 would be changed from the tip of the nozzle to sphere surface through traveling the large open space. It is deduced that the ambient oxygen partial pressure around the sphere might be controlled to some extent, even though the concentration field was not calculated yet. On the contrary, an oxygen sensor attached to the sucking nozzle might not detect correct value of Po_2 of the gas which reached the sphere, because the nozzle sucks also the inlet gas diluted by a main body of the chamber gas, as shown by a dotted-line in **Fig.7a**. This is due to misalignment of the suction nozzle, as shown **Fig. 1b**.

Under the 1.5 G condition, the strong buoyancy convection was confirmed, as shown in Fig. 7b. This enforces the gas to rise along the gravity direction; the inlet gas is unable to reach the sphere surface by strong convection. The suction nozzle collects its ambient gas, which does not touch the sphere surface and does not come from the inlet nozzle. This means that we can neither control the oxygen partial pressure of sphere surface by inlet gas nor measure the surface oxygen partial pressure through suctioning.

3.3 Numerical Procedure (Proposed Model)

According to the CFD results for the conventional control method, the Po_2 control and measurement are impossible for the

Fig. 8 Numerical model: gas flows from the top of the cylinder to a sample surface and is out at the bottom.

PFLEX system. We propose the following new Po_2 control model, which can recover the missing part of the conventional model. For the new model, the glass tube is employed inside the coil like a ground-based experiment system. Controlled gas flows from top of the tube and Po_2 is observed at the bottom.

Figure 8 shows the numerical model of the gas flow from the top to the bottom of the cylinder. A cylinder mimics the employed glass tube. A high temperature solid is placed at the center of the tube. Controlled gas flows from top surface of the cylinder and the bottom surface is free.

The governing equations for the motion of an incompressible

fluid flow are similar to that of the conventional model except for the advective-difussion equation of oxygen concentration. By adding the following equation to the governing equation system of present model;

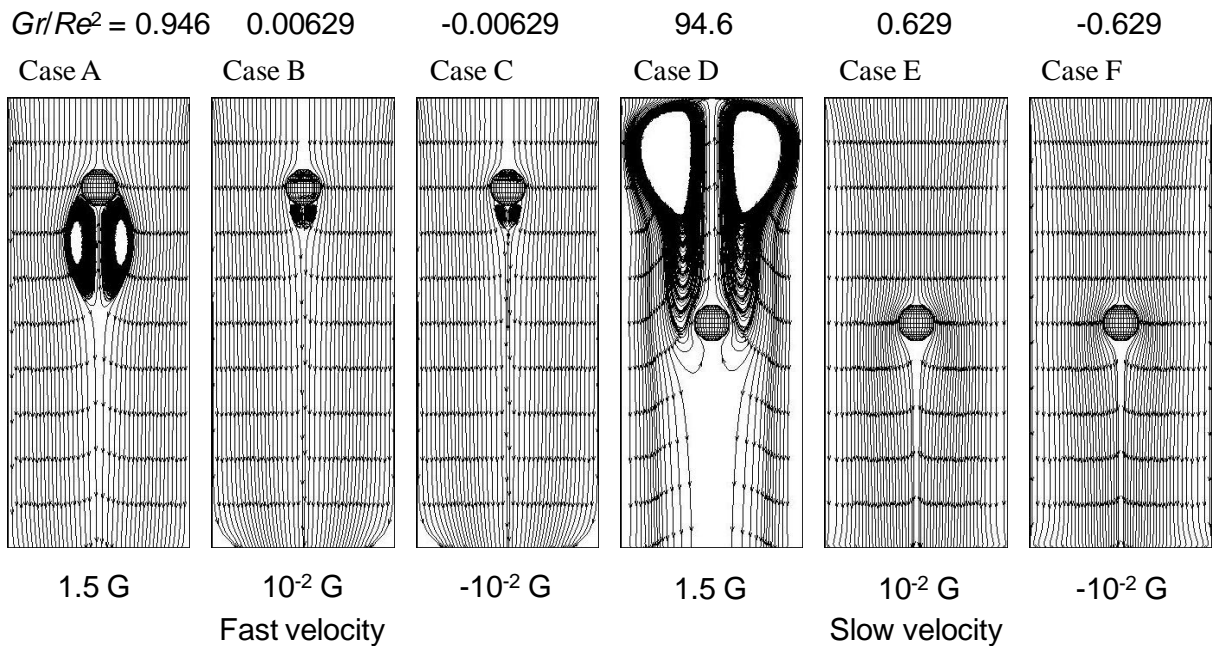$$\frac{\partial c}{\partial t} = -\nabla \cdot (\mathbf{u}c) + \frac{1}{Re \cdot Sc} \nabla^2 c \tag{5}$$

Here, The Scmidt number is defined as eq. (6), where Do_2 is the concentration diffusivity;

$$Sc = \frac{\nu}{Do_2} \tag{6}$$

The computational domain has a radius of 2.5 D and a length of 12.5 D as shown in Fig. 8. No-slip boundary condition is applied at side surface. The forced flow is applied at top surface and the Sommerfeld boundary condition is applied at the bottom surface, which is free spatial boundary condition. The number of computational cells is 32 $\times$ 36 $\times$ 90 for the radial, azimuthal and axial direction, respectively. Equally spaced cells are adopted for all directions. Six cases of steady flows under the 1.5 G, 10^{-2} G and 10^{-2} G conditions are simulated for inlet gas velocity of both 0.5 m/s and 0.05 m/s.

3.4 Numerical Result (Proposed Model)

Figure 9 shows the result of streamlines for each parameter. For the Cases A to C and the Cases D to F, the Reynolds numbers are 141 and 14, respectively. For each case, different gravitational acceleration was given. The characteristic

$Gr/Re^2 = 0.946$	0.00629	-0.00629	94.6	0.629	-0.629
Case A	Case B	Case C	Case D	Case E	Case F

1.5 G	10^{-2} G	-10^{-2} G	1.5 G	10^{-2} G	-10^{-2} G
Fast velocity			Slow velocity		

Fig. 9 The results of streamline analysis for each case. For the cases A and C (*Re* = 141), gravitational acceleration is different from each other. For the cases D and F (*Re* = 14), gravitational acceleration is different from each other.
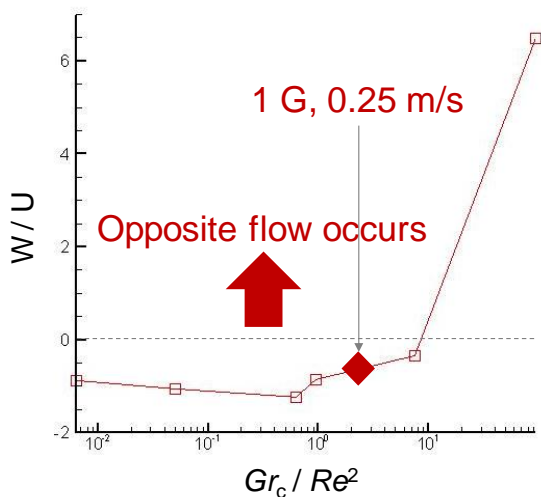
Fig. 10 Axial velocity above the sphere 1 D by Gr/Re^2 for the each case of CFD result. The buoyancy convection will occur in range of axial velocity by characteristic velocity > 0.

parameter Gr/Re^2 is calculated for each case which indicates the ratio of buoyancy convection to inertial force.

For the case A, the buoyancy convection is not confirmed, whereas for the case D, the strong buoyancy convection is confirmed. The difference is due to the inlet gas velocity. The gas velocity of 0.5 m/s enables to suppress the buoyancy effect, whereas the gas velocity of 0.05 m/s does not suppress this effect. All these results are similar to each other for the cases B and C as well as for E and F. This implies that we can neglect the g-jitter effect on the fluid dynamics.

According to these results, the parameter Gr/Re^2 is possible to predict whether the buoyancy convection occurs or not. **Figure 10** shows the axial velocity at the 1 D above the sphere as a function of the parameter Gr/Re^2; the results for the cases of $Re = 50$ under $g = 1.5$ G and 10^{-2} G were added. It was found that the opposite flow occurs for range from Gr/Re^2 10 to 94.6.

4. Summary

From the viewpoint of system engineering, we analyzed the PFLEX (Parabolic Flight Levitation EXperimental facility) experiment for the measurement of thermophysical property under the microgravity condition on board the aircraft. This is the first trial of applying a system engineering method to a parabolic flight experiment. By decomposing the PFLEX experiment system into subsystem and component levels, the attitude of the aircraft, gravity level, chamber, measurement system and human activity, which are on physically different levels to each other, can be described and considered as the same level of events. Through this analysis, an optimized condition was obtained so as to fully utilize a microgravity condition, overcoming constraints such as a limit of the experimenter's activity, inevitable gravity change as high as 1.5 G and so on.

For the conventional geometry of the chamber system under the microgravity condition, the inlet gas wrapped a sphere sample and flew over the sphere and reached the opposite wall. This suggests that oxygen partial pressure at the sample surface might be controlled by introducing a gas with a certain oxygen concentration. However, Po_2 at the surface of the sphere cannot be observed yet. Thus, we propose the new model employing a quartz glass tube. It was found that the buoyancy convection will vanish, if appropriate gas inlet velocity is adopted over 0.5 m/s. Furthermore, we indicate that the CFD program is more effective than empirical one aboard the aircraft, so as to verify the model for Po_2 control.

References

1) S. Nakamura, T. Hibiya and F. Yamamoto: Microgravity Science and Technology, **5** (1992) 156.
2) J. Kim, K. N. Kim, S. H. Won, O. Fujita, J. Takahashi and S. H. Chung: Combust. Flame, **145** (2006) 181.
3) S. Ozawa, M. Watanabe, Y. Kiyamura, K. Morohoshi, Y. Aoyagi, T. Mitsuhiro, T. Matsumoto, M. Adachi, A. Mizuno, H. Fujii and T. Hibiya: J. Jpn. Soc. Microgravity Appl., **27** (2010) 215..
4) T. Hibiya: J. Jpn. Soc. Microgravity Appl., **25** (2008) 177.
5) See for example, 'Final Reports of TR-Rocket No. 4 Microgravity Experiments', National Space Development Agency of Japan, NASDA-TMR 960018 (1996) (in Japanese).
6) See for example, J. Jpn. Soc. Microgravity Appl., Special Issue: Microgravity Experiments Using Airplane, **18** (2001) (in Japanese).
7) T. Masaki, T. Fukazawa, S. Matsumoto, T. Itami and S. Yoda, Measurement Science and Technology, **16** (2005) 327.
8) D. L. Cummings and D. A. Blackburn: Journal of Fluid Mechanics, **224** (1991) 395.
9) K. Fukagata and N. Kasagi: Journal of Computational Physics, **181** (2002) 478.